

Radiosynthesis of [¹¹C]LY2795050 for Preclinical and Clinical PET Imaging Using Cu(II)-Mediated Cyanation

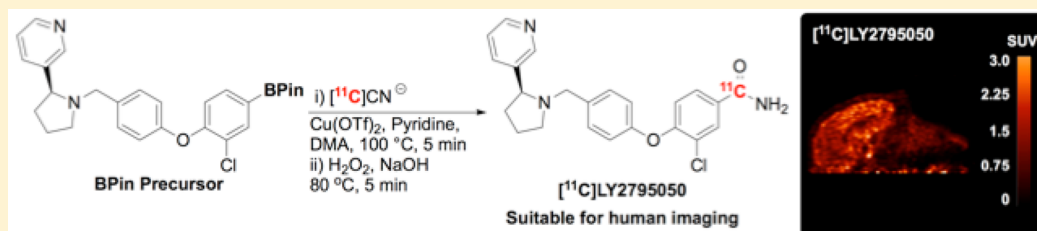
Lingyun Yang,^{†,‡} Allen F. Brooks,[†] Katarina J. Makaravage,[§] Huibin Zhang,[‡] Melanie S. Sanford,^{*,§} Peter J. H. Scott,^{*,†} and Xia Shao^{*,†}

[†]Department of Radiology, University of Michigan, Ann Arbor, Michigan 48109, United States

[‡]Center of Drug Discovery, State Key Laboratory of Natural Medicines, China Pharmaceutical University, Nanjing 211198, P.R. China

[§]Department of Chemistry, University of Michigan, Ann Arbor, Michigan 48109, United States

Supporting Information



ABSTRACT: Copper-mediated ¹¹C-cyanation reactions have enabled the synthesis of PET radiotracers from a range of readily available precursors and avoid the need to use more toxic Pd catalysts. In this work we adapt our recently developed ¹¹C-cyanation of arylpinacolboronate (BPin) esters for the cGMP synthesis of [¹¹C]LY2795050, a selective antagonist radiotracer for the kappa opioid receptor (KOR). [¹¹C]LY2795050 was synthesized in 6 ± 1% noncorrected radiochemical yield (based on [¹¹C]HCN, *n* = 3) using an automated synthesis module. Quality control testing confirmed the suitability of doses for preclinical and clinical PET imaging (radiochemical purity >99%; specific activity >900 mCi/μmol; residual Cu < 0.1 μg/mL). PET imaging was conducted in rodent and nonhuman primates, showing good brain uptake of [¹¹C]LY2795050 and the expected distribution of KOR. Analogous imaging with [¹¹C]carfentanil (a selective mu opioid receptor (MOR) radiotracer) revealed the anticipated regional differences in MOR and KOR distribution in the primate brain.

KEYWORDS: Positron emission tomography imaging, kappa opioid receptor, carbon-11, cyanation

Opioid receptors are involved in a variety of neuropsychiatric diseases and remain popular targets for imaging and drug development.¹ These receptors were first imaged in humans using positron emission tomography (PET) in the 1980s.² Since these early studies, significant work has been undertaken to develop radiotracers for quantifying the major opioid receptor subtypes (mu, delta, kappa, ORL-1).³ Given that popular opioid pain killers such as morphine, codeine, and fentanyl all act preferentially at mu opioid receptors (MORs),^{4,5} significant work has been undertaken to understand the pharmacology of this receptor. For example, we have used [¹¹C]carfentanil ([¹¹C]CFN) for decades with clinical colleagues to image the mu opioid system.⁶

Mu opioid agonists are some of the most effective pain killers used in modern medicine.⁷ However, the abuse of opioids including prescription pain relievers, synthetic opioids, and street drugs, has led to a serious crisis in the United States.⁸ The Centers for Disease Control estimate that about 72,000 Americans died of drug overdoses in 2017 alone, with opioids implicated in 49,000 of these deaths.⁹ This crisis has provided strong motivation to develop opioid painkillers without undesirable side effects and that do not lead to

dependence. Since analgesia is associated with all of the opioid receptor subtypes, but dependence and other side effects such as respiratory depression are mostly attributed to mu receptors, there is enormous interest in developing drugs (and PET radiotracers) that are selective for the other opioid subtypes.¹⁰ The kappa opioid receptor (KOR) structure has been recently revealed,¹¹ and this is expected to spur development of new drugs for this target.¹² Reflecting this, our clinical colleagues desire access to a KOR-selective PET radiotracer manufactured according to current Good Manufacturing Practice (cGMP) and suitable for clinical use.

To date, several KOR antagonist radiotracers for PET imaging have been reported.^{13–20} For clinical translation, we selected [¹¹C]LY2795050 ([¹¹C]1) since it has high affinity (in vitro *K_i* = 0.72 nM; in vivo *K_d* = 0.028 nM) and good selectivity for KOR (*μ*/*κ* = 11; *δ*/*κ* = 132).^{20–23} Furthermore, the first evaluation of [¹¹C]LY2795050 in human subjects demonstrated the feasibility of using this radiotracer to image

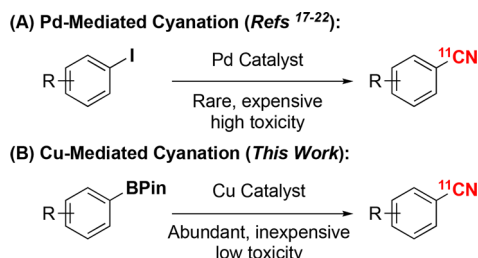
Received: October 3, 2018

Accepted: November 13, 2018

Published: November 13, 2018

KOR.²⁰ However, all of the previously reported syntheses of [¹¹C]LY2795050 employed Pd-mediated cyanation reactions (Scheme 1A).^{17–22} These are undesirable as Pd is expensive

Scheme 1. Inspiration for the Synthesis of [¹¹C]LY2795050 via Cu-Mediated ¹¹C-Cyanation



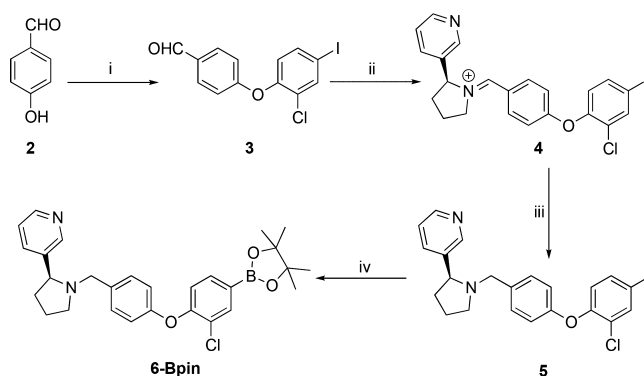
(Pd₂dba₃ = \$37,273/mol²⁴) and has a relatively high toxicity with a low permitted daily exposure in drugs (≤10 μg/day for parenteral administration²⁵).

Copper-mediated radiolabeling reactions represent an attractive alternative to their palladium counterparts because the catalysts are comparatively inexpensive (Cu(OTf)₂ = \$4,686/mol²⁴), and Cu is significantly less toxic than Pd, reflected in a much higher permitted daily exposure limit (≤340 μg/day for parenteral administration²⁵). We^{26–30} and others^{31–33} have recently shown that Cu-mediated ¹⁸F-fluorination and ¹¹C-cyanation reactions can be used to label bioactive molecules from diverse aryl precursors with fluorine-18 and carbon-11, respectively. In this report, we describe the automated cGMP production of [¹¹C]LY2795050 doses suitable for clinical use via the Cu-mediated cyanation of an arylpinacolboronate (BPin) ester precursor with [¹¹C]cyanide (Scheme 1B).³⁴ With production batches in hand, we compared KOR distribution in nonhuman primates imaged with [¹¹C]LY2795050 to MOR distribution imaged with [¹¹C]CFN.

In our recent report of Cu-mediated ¹¹C-cyanation reactions, we demonstrated that a range of precursors were compatible with the method, including BPin esters.³⁰ Thus, to explore the radiosynthesis of [¹¹C]LY2795050, we initially prepared arylboronate ester precursor (**6-Bpin**) as shown in Scheme 2. The condensation between 4-hydroxybenzaldehyde **2** and 2-chloro-1-fluoro-4-iodobenzene afforded aldehyde **3** in 18% yield. The aldehyde was converted to iminium **4** with (S)-3-(pyrrolidin-2-yl)pyridine, followed by reduction to form **5** in 85% yield from **3**. The desired precursor **6-Bpin** was then obtained in 65% yield by treating **5** with bis(pinacolato)diboron. In order to confirm the identity of the radiolabeled product, unlabeled LY2795050 reference standard was also synthesized (see Supporting Information).

Initial manual labeling reactions were conducted to evaluate the potential for labeling [¹¹C]LY2795050 using a Cu-mediated ¹¹C-cyanation. One M KOH was used to trap [¹¹C]HCN, remove residual NH₃ used in its production (since NH₃ can be detrimental to downstream radiochemical reactions), and convert it to [¹¹C]KCN as previously described.³⁵ Small aliquots of this solution were subjected to our standard conditions (**6-BPin**, Cu(OTf)₂, and pyridine) which, following hydrolysis with 30% H₂O₂ and 5.0 M NaOH, afforded 39% radiochemical conversion (RCC) to [¹¹C]-LY2795050 ([¹¹C]**1**) (Table 1, entry 1). When we translated this reaction to an automated synthesis module, we tried to

Scheme 2. Synthesis of Arylboronate Ester Precursor (**6-Bpin**).^a



^aReagents and conditions: (i) 2-chloro-1-fluoro-4-iodobenzene, K₂CO₃, Cs₂CO₃, DMF, 12 h, 140 °C, 18%; (ii) (S)-3-(pyrrolidin-2-yl)pyridine, 1,2-DCE, 24 h, 65 °C; (iii) NaBH(OAc)₃, AcOH, 24 h, 65 °C, 85% (over 2 steps from **3**); (iv) bis(pinacolato)diboron, Pd(dppf)Cl₂, KOAc, DMSO, 12 h, 85 °C, 65%.

duplicate this manual reaction by adding 1 M aqueous KOH (0.2 mL) to the reactor to trap [¹¹C]HCN and convert it to [¹¹C]KCN. However, there was a marked decrease in RCC, probably due to the deactivation of the Cu under strongly basic conditions (entry 2). We next tested use of Pt wire coated with 1 M KOH to trap [¹¹C]HCN and convert it to [¹¹C]KCN as previously described,³⁵ and obtained comparable conversion to [¹¹C]**1** for the manual reaction (entry 3). This approach, while effective, does require more time and steps than direct use of [¹¹C]HCN from the cyclotron, which is problematic when considering the short half-life of ¹¹C (20 min). If residual NH₃ were not detrimental to the labeling of **6-Bpin**, we could simplify and speed up the synthesis by removing the Pt wire and bubbling [¹¹C]HCN directly into the reaction mixture. This proved to be the case, and bubbling [¹¹C]HCN directly into a solution of Cu(OTf)₂ and pyridine (15 equiv) in DMA (0.25 mL) demonstrated compatibility with NH₃. Conversion to [¹¹C]**1** correlated with the equivalents of Cu utilized (entries 4–6). A further boost in RCC was achieved when Cu was added after [¹¹C]HCN delivery (entries 7 and 8). The addition of exogenous H₂O (0.05 mL), which was beneficial for ¹¹C-cyanation with [¹¹C]KCN in our previous work,³⁰ was not necessary for the synthesis of [¹¹C]LY2795050 (entry 8), likely because HCN is more soluble in DMA than KCN. Thus, we moved forward using the method involving trapping with pyridine in DMA (entry 7).

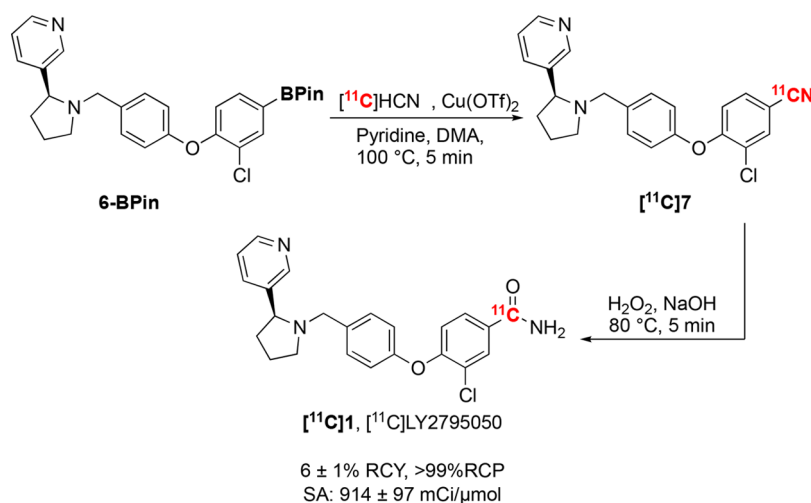
With an optimized radiosynthesis in hand, we next automated the full synthesis, purification, and reformulation of [¹¹C]LY2795050 to qualify the method for cGMP production of animal and clinical doses (Scheme 3). No carrier added [¹¹C]HCN (~800 mCi) was bubbled into a mixture of pyridine (15 equiv) in DMA (0.25 mL). Cu(OTf)₂ (4 equiv) was then added, followed by **6-Bpin** (1 equiv), and the reaction was heated at 100 °C for 5 min to generate cyano intermediate [¹¹C]**7**. Hydrolysis to generate [¹¹C]LY2795050 ([¹¹C]**1**) was accomplished by treating [¹¹C]**7** with 30% H₂O₂ (0.2 mL) and 5.0 M NaOH (0.2 mL) at 80 °C for 5 min. The reaction mixture was then diluted with acetic acid (0.4 mL) and purified by semipreparative HPLC (column: Phenomenex Prodigy C8, 10 μm, 150 × 10 mm; mobile phase: 25:75 MeCN:H₂O, 100 mM NH₄OAc, 1.0% acetic acid, pH = 4.8;

Table 1. Reaction Optimization Studies



Entry	Trapping Method	Cu eq	RCC ^a
1	None	2	39 ± 4% ^b
2	1 M KOH	2	5%
3	Pt wire coated with KOH	2	31%
4	Cu(OTf) ₂ /pyridine in DMA	2	20%
5	Cu(OTf) ₂ /pyridine in DMA	3	25%
6	Cu(OTf) ₂ /pyridine in DMA	4	30%
7	Pyridine in DMA	4	47%
8	H ₂ O/pyridine in DMA	4	50%

^aRCC = radiochemical conversion over 2 steps. ^bn = 2.

Scheme 3. Radiosynthesis of [¹¹C]LY2795050

UV = 254 nm, flow rate = 5.0 mL/min). The peak corresponding to [¹¹C]LY2795050 ($t_R \sim 5\text{--}7$ min, see Figure S3 in the Supporting Information) was collected and reformulated using a C18 solid-phase extraction cartridge to afford formulated doses of [¹¹C]LY2795050 (48 ± 10 mCi, $n = 3$). The total synthesis time was approximately 45 min from end-of-bombardment. The nondecay corrected radiochemical yield (RCY) was $6 \pm 1\%$, based upon [¹¹C]HCN. Radiochemical purity (RCP) was >99%, and specific activity was 914 ± 97 mCi/μmol ($n = 3$). Doses from three validation runs were submitted for quality control (QC) testing, and all doses met or exceeded release criteria for clinical application at the University of Michigan, including purity, sterility, and residual solvent analysis (Table 2). Doses produced used Cu-mediated reactions also need to be free of residual Cu if they are to be used in the clinic. Samples from each of the qualification runs were submitted for inductively coupled plasma mass spectrometry (ICP-MS) analysis and were found to contain residual Cu below the limit of quantification (<100 ppb), well below the established limit for Cu.²⁵

With a qualified synthesis in hand, we next performed preclinical PET imaging with [¹¹C]LY2795050. Initial studies were performed in rodents (see Supporting Information) and

Table 2. QC Data for Three Validation Runs

QC Test	Specifications	Lot 1	Lot 2	Lot 3
Visual Inspection	Clear, colorless, no ppt	Pass	Pass	Pass
pH	4.5–7.5	5.0	5.0	5.0
RCP	≥90%	>99	>99	>99
Conc.	≥3mCi/mL	4.1	5.9	4.4
Radiochemical-ID	RRT: 0.9–1.1	1.0	1.0	1.0
Radionuclidic-ID	$t_{1/2}$: 20 ± 2 min	20.6	20.0	19.8
Filter integrity	Bubble point ≥45 psi	50	48	47
Endotoxins	≤17.5 EU/mL	≤2.00	≤2.00	≤2.00
Sterility	No microbial growth	Pass	Pass	Pass
Residual Cu	<34 μg/mL	<0.1	<0.1	<0.1

confirmed good brain uptake of the radiotracer and suitability for *in vivo* imaging. Lastly, with access to both [¹¹C]LY2795050 for KOR and [¹¹C]CFN for MOR (prepared as previously described⁶), we compared the regional brain distribution of the two receptors in nonhuman primates (Figure 1). PET imaging with both radiotracers was performed in the same rhesus monkey, and regions-of-interest were established and used to generate time-activity curves (TACs). [¹¹C]LY2795050 displayed good brain uptake (peak SUV

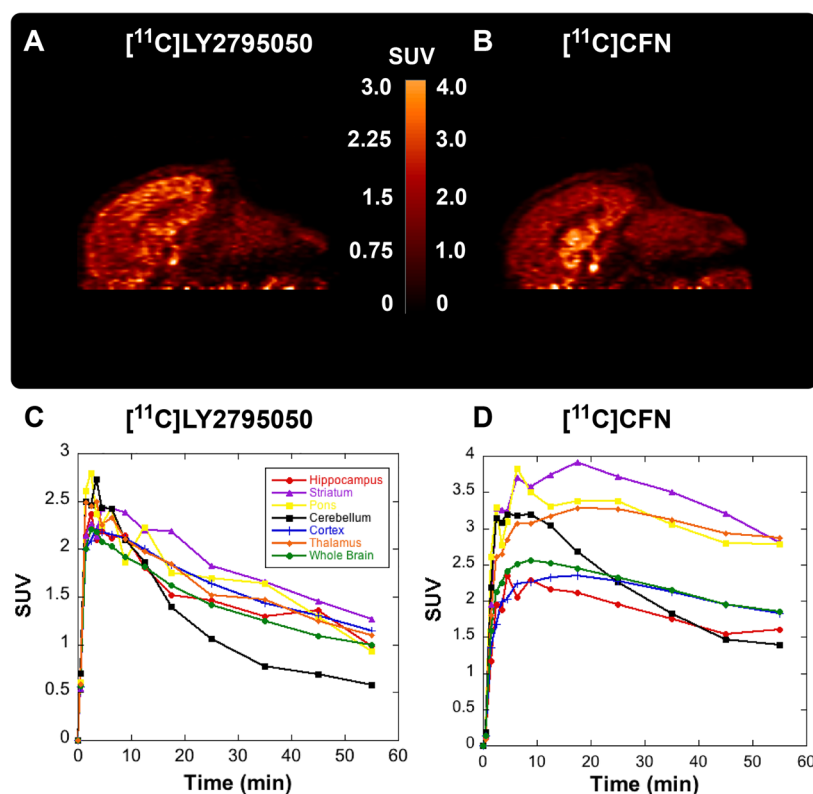


Figure 1. Summed sagittal primate PET images of [11C]LY2795050 (A) and [11C]CFN (B) 0–60 min after injection of the radiotracer and associated time-activity curves (C and D). (High resolution TACs are provided in the Supporting Information, see Figures S6 and S7).

~3.5–4.5 min in selected brain regions) and a heterogeneous distribution pattern (striatum > cortex ~ thalamus > cerebellum), consistent with previous reports of KOR distribution in nonhuman primates.³⁶ MOR imaging with [11C]CFN revealed different distribution. After the fast initial uptake (peak SUV at 6.25–8.75 min in selected regions), [11C]CFN uptake in cerebellum washed out gradually, but the tracer was retained well in striatum, thalamus, and pons. The difference between imaging with [11C]LY2795050 and [11C]CFN is consistent with the differences in distribution of KOR and MOR in the primate brain.^{36–39}

In summary, we report the first validation of our Cu-mediated cyanation of BPIn esters for the cGMP synthesis of a PET radiotracer for preclinical and clinical applications. The synthesis of [11C]LY2795050, a PET radiotracer for the KOR, was fully automated using a commercial radiochemistry synthesis module. Doses met all QC criteria for preclinical and clinical use and were used to image rodents and nonhuman primates. Comparison with [11C]CFN imaging of MOR identified regional brain distribution differences consistent with the known distribution of opioid receptors in primates. We expect to initiate clinical imaging studies with [11C]LY2795050 in the near future.

■ ASSOCIATED CONTENT

📄 Supporting Information

The Supporting Information is available free of charge on the ACS Publications website at DOI: 10.1021/acsmchemlett.8b00460.

Full experimental details; copies of ¹H NMR and ¹³C NMR spectra, as well as HRMS, for novel and/or key compounds (**1**, **6-BPin** and **6-SnMe₃**); copies of ¹NMR

spectra and HRMS for other known compounds synthesized; procedures and HPLC chromatograms for radiochemical syntheses and quality control; protocols for animal PET imaging studies. (PDF)

■ AUTHOR INFORMATION

Corresponding Authors

*E-mail: mssanfor@umich.edu.

*E-mail: pjhscott@umich.edu.

*E-mail: xshao@umich.edu.

ORCID

Allen F. Brooks: 0000-0003-3773-3024

Katarina J. Makaravage: 0000-0002-1225-5305

Melanie S. Sanford: 0000-0001-9342-9436

Peter J. H. Scott: 0000-0002-6505-0450

Xia Shao: 0000-0002-7291-2477

Author Contributions

The manuscript was written through contributions of all authors and all authors have given approval to the final version of the manuscript.

Funding

This work was supported by NIH (R01EB021155, M.S.S. and P.J.H.S.) and the China Scholarship Council (201607060008, L.Y. and P.J.H.S.).

Notes

The authors declare no competing financial interest.

■ ACKNOWLEDGMENTS

The authors thank Jenelle Stauff, Janna Arteaga, and Phillip Sherman for conducting animal studies and Bradford Henderson for assistance with QC testing.

■ ABBREVIATIONS

CFN, carfentanil; 1,2-DCE, 1,2-dichloroethane; DMA, *N,N*-dimethylacetamide; DMF, *N,N*-dimethylformamide; DMSO, dimethyl sulfoxide; DOR, delta opioid receptor; HPLC, high-performance liquid chromatography; KOR, kappa opioid receptor; MOR, mu opioid receptor; RCC, radiochemical conversion; RCP, radiochemical purity; RCY, radiochemical yield; ROI, regions-of-interest; SUV, standardized uptake value; PET, positron emission tomography.

■ REFERENCES

- (1) Waldhoer, M.; Bartlett, S. E.; Whistler, J. L. Opioid receptors. *Annu. Rev. Biochem.* **2004**, *73*, 953–990.
- (2) For a historical overview, see: van Waarde, A.; Absalom, A. R.; Visser, A. K. D.; Dierckx, A. J. O. Positron emission tomography (PET) imaging of opioid receptors. In Dierckx, R., Otte, A., de Vries, E., van Waarde, A., Luiten, P., Eds.; *PET and SPECT of Neurobiological Systems*; Springer, Berlin, Heidelberg, 2014.
- (3) Lever, J. R. PET and SPECT imaging of the opioid system: receptors, radioligands and avenues for drug discovery and development. *Curr. Pharm. Des.* **2007**, *13*, 33–49.
- (4) Mignat, C.; Wille, U.; Ziegler, A. Affinity profiles of morphine, codeine, dihydrocodeine and their glucuronides at opioid receptor subtypes. *Life Sci.* **1995**, *56*, 793–799.
- (5) Maguire, P.; Tsai, N.; Kamal, J.; Cometta-Morini, C.; Upton, C.; Loew, G. Pharmacological profiles of fentanyl analogs at μ , δ and κ opiate receptors. *Eur. J. Pharmacol.* **1992**, *213*, 219–225.
- (6) Blecha, J. E.; Henderson, B. D.; Hockley, B. G.; VanBrocklin, H. F.; Zubieta, J. K.; DaSilva, A. F.; Kilbourn, M. R.; Koeppe, R. A.; Scott, P. J. H.; Shao, X. An updated synthesis of [^{11}C]carfentanil for positron emission tomography (PET) imaging of the μ -opioid receptor. *J. Labelled Compd. Radiopharm.* **2017**, *60*, 375–380.
- (7) Pasternak, G.; Pan, Y.-X. Mu opioid receptors in pain management. *Acta Anaesthesiol. Taiwan.* **2011**, *49*, 21–25.
- (8) Skolnick, P. The opioid epidemic: crisis and solutions. *Annu. Rev. Pharmacol. Toxicol.* **2018**, *58*, 143–159.
- (9) Durkin, E. US drug overdose deaths rose to record 72,000 last year, data reveals. The Guardian, Aug 16th, 2018, <https://www.theguardian.com/us-news/2018/aug/16/us-drug-overdose-deaths-opioids-fentanyl-cdc>; accessed 18-Sept-2018.
- (10) Fudin, J. Opioid agonists, partial agonists, antagonists: oh my!. *Pharmacy Times*; 2018, <https://www.pharmacytimes.com/contributor/jeffrey-fudin/2018/01/opioid-agonists-partial-agonists-antagonists-oh-my>; accessed 18-Sept-2018.
- (11) Che, T.; Majumdar, S.; Zaidi, S. A.; Ondachi, P.; McCorvy, J. D.; Wang, S.; Mosier, P. D.; Upreti, R.; Vardy, E.; Krumm, B. E.; Han, G. W.; Lee, M. Y.; Pardon, E.; Steyaert, J.; Huang, X. P.; Strachan, R. T.; Tribo, A. R.; Pasternak, G. W.; Carroll, F. I.; Stevens, R. C.; Cherezov, V.; Katritch, V.; Wacker, D.; Roth, B. L. Structure of the nanobody-stabilized active state of the kappa opioid receptor. *Cell* **2018**, *172*, 55–67.
- (12) Lalanne, L.; Ayranci, G.; Kieffer, B. L.; Lutz, P. E. The kappa opioid receptor: from addiction to depression, and back. *Front. Mol. Psychiatry* **2014**, *5*, No. 170.
- (13) Poisnel, G.; Oueslati, F.; Dhilly, M.; Delamare, J.; Perrio, C.; Debruyne, D.; Barre, L. [^{11}C]-MeJDTic: a novel radioligand for kappa-opioid receptor positron emission tomography imaging. *Nucl. Med. Biol.* **2008**, *35*, S61–S69.
- (14) Schmitt, S.; Delamare, J.; Tirel, O.; Fillesoye, F.; Dhilly, M.; Perrio, C. *N*-[^{18}F]-FluoropropylJDTic for kappa-opioid receptor PET imaging: Radiosynthesis, pre-clinical evaluation, and metabolic investigation in comparison with parent JDTic. *Nucl. Med. Biol.* **2017**, *44*, 50–61.
- (15) Li, S.; Cai, Z.; Zheng, M. Q.; Holden, D.; Naganawa, M.; Lin, S. F.; Ropchan, J.; Labaree, D.; Kapinos, M.; Lara-Jaime, T.; Navarro, A.; Huang, Y. Novel ^{18}F -Labeled κ -Opioid Receptor Antagonist as PET Radiotracer: Synthesis and In Vivo Evaluation of ^{18}F -LY2459989 in Nonhuman Primates. *J. Nucl. Med.* **2018**, *59*, 140–146.
- (16) Cai, Z.; Li, S.; Pracitto, R.; Navarro, A.; Shirali, A.; Ropchan, J.; Huang, Y. Fluorine-18-Labeled Antagonist for PET Imaging of Kappa Opioid Receptors. *ACS Chem. Neurosci.* **2017**, *8*, 12–16.
- (17) Kim, S. J.; Zheng, M. Q.; Nabulsi, N.; Labaree, D.; Ropchan, J.; Najafzadeh, S.; Carson, R. E.; Huang, Y.; Morris, E. D. Determination of the in vivo selectivity of a new kappa-opioid receptor antagonist PET tracer ^{11}C -LY2795050 in the rhesus monkey. *J. Nucl. Med.* **2013**, *54*, 1668–1674.
- (18) Zheng, M. Q.; Nabulsi, N.; Kim, S. J.; Tomasi, G.; Lin, S. F.; Mitch, C.; Quimby, S.; Barth, V.; Rash, K.; Masters, J.; Navarro, A.; Seest, E.; Morris, E. D.; Carson, R. E.; Huang, Y. Synthesis and evaluation of ^{11}C -LY2795050 as a kappa-opioid receptor antagonist radiotracer for PET imaging. *J. Nucl. Med.* **2013**, *54*, 455–463.
- (19) Placzek, M. S.; Schroeder, F. A.; Che, T.; Wey, H.-Y.; Neelamegam, R.; Wang, C.; Roth, B. L.; Hooker, J. M. Discrepancies in kappa opioid agonist binding revealed through PET imaging. *ACS Chem. Neurosci.* **2018**, DOI: 10.1021/acschemneuro.8b00293.
- (20) Naganawa, M.; Zheng, M. Q.; Nabulsi, N.; Tomasi, G.; Henry, S.; Lin, S. F.; Ropchan, J.; Labaree, D.; Tauscher, J.; Neumeister, A.; Carson, R. E.; Huang, Y. Kinetic modeling of ^{11}C -LY2795050, a novel antagonist radiotracer for PET imaging of the kappa opioid receptor in humans. *J. Cereb. Blood Flow Metab.* **2014**, *34*, 1818–1825.
- (21) Naganawa, M.; Zheng, M. Q.; Henry, S.; Nabulsi, N.; Lin, S. F.; Ropchan, J.; Labaree, D.; Najafzadeh, S.; Kapinos, M.; Tauscher, J.; Neumeister, A.; Carson, R. E.; Huang, Y. Test-retest reproducibility of binding parameters in humans with ^{11}C -LY2795050, an antagonist PET radiotracer for the κ opioid receptor. *J. Nucl. Med.* **2015**, *56*, 243–248.
- (22) Lee, H. G.; Milner, P. J.; Placzek, M. S.; Buchwald, S. L.; Hooker, J. M. Virtually instantaneous, room-temperature [^{11}C]cyanation using biaryl phosphine Pd(0) complexes. *J. Am. Chem. Soc.* **2015**, *137*, 648–651.
- (23) Mitch, C. H.; Quimby, S. J.; Diaz, N.; Pedregal, C.; de la Torre, M. G.; Jimenez, A.; Shi, Q.; Canada, E. J.; Kahl, S. D.; Statnick, M. A.; McKinzie, D. L.; Benesh, D. R.; Rash, K. S.; Barth, V. N. Discovery of aminobenzylxyarylamides as κ opioid receptor selective antagonists: application to preclinical development of a κ opioid receptor antagonist receptor occupancy tracer. *J. Med. Chem.* **2011**, *54*, 8000–8012.
- (24) www.sigmaaldrich.com, accessed 18-Sept-2018.
- (25) Guidelines for Elemental Impurities. http://www.ich.org/fileadmin/Public_Web_Site/ICH_Products/Guidelines/Quality/Q3D/Q3D_Step_4.pdf; accessed 18-Sept-2018.
- (26) Ichiishi, N.; Brooks, A. F.; Topczewski, J. J.; Rodnick, M. E.; Sanford, M. S.; Scott, P. J. H. Copper-catalyzed [^{18}F]fluorination of (mesityl)ArylIodonium Salts. *Org. Lett.* **2014**, *16*, 3224–3227.
- (27) Mossine, A. V.; Brooks, A. F.; Makaravage, K. J.; Miller, J. M.; Ichiishi, N.; Sanford, M. S.; Scott, P. J. H. Synthesis of [^{18}F]arenes via the copper-mediated [^{18}F]fluorination of boronic acids. *Org. Lett.* **2015**, *17*, 5780–5783.
- (28) Makaravage, K. J.; Brooks, A. F.; Mossine, A. V.; Sanford, M. S.; Scott, P. J. H. Copper-mediated radiofluorination of arylstannanes with [^{18}F]KF. *Org. Lett.* **2016**, *18*, 5440–5443.
- (29) McCamant, M. S.; Thompson, S.; Brooks, A. F.; Krska, S. W.; Scott, P. J. H.; Sanford, M. S. Cu-Mediated C-H ^{18}F -fluorination of electron-rich (hetero)arenes. *Org. Lett.* **2017**, *19*, 3939–3942.
- (30) Makaravage, K. J.; Shao, X.; Brooks, A. F.; Yang, L.; Sanford, M. S.; Scott, P. J. H. Copper(II)-mediated [^{11}C]cyanation of arylboronic acids and arylstannanes. *Org. Lett.* **2018**, *20*, 1530–1533.
- (31) Tredwell, M.; Preshlock, S. M.; Taylor, N. J.; Gruber, S.; Huiban, M.; Passchier, J.; Mercier, J.; Génicot, C.; Gouverneur, V. A general copper-mediated nucleophilic ^{18}F fluorination of arenes. *Angew. Chem., Int. Ed.* **2014**, *53*, 7751–7755.
- (32) Zlatopolskiy, B. D.; Zischler, J.; Krapf, P.; Zarrad, F.; Urusova, E. A.; Kordys, E.; Endepols, H.; Neumaier, B. Copper-mediated aromatic radiofluorination revisited: efficient production of PET tracers on a preparative scale. *Chem. - Eur. J.* **2015**, *21*, 5972–5979.

(33) Ma, L.; Placzek, M. S.; Hooker, J. M.; Vasdev, N.; Liang, S. H. [¹¹C]Cyanation of arylboronic acids in aqueous solution. *Chem. Commun.* **2017**, 53, 6597–6600.

(34) The stannane precursor (**6-SnMe₃**) was also compatible with this method as detailed in the Supporting Information. However, RCC was notably higher when using the BPin precursor in a side-by-side comparison (50% vs 31%) and so we selected **6-BPin** to qualify for clinical production of [¹¹C]LY2795050.

(35) Xing, J.; Brooks, A. F.; Fink, D.; Zhang, H.; Piert, M. R.; Scott, P. J. H.; Shao, X. High-yielding automated convergent synthesis of no-carrier-added [¹¹C-carbonyl]-labeled amino acids using the strecker reaction. *Synlett* **2017**, 27, 371–375.

(36) Ragen, B. J.; Freeman, S. M.; Laredo, S. A.; Mendoza, S. P.; Bales, K. L. μ and κ opioid receptor distribution in the monogamous titi monkey (*Callicebus cupreus*): Implications for social behavior and endocrine functioning. *Neuroscience* **2015**, 290, 421–434.

(37) Mansour, A.; Fox, C. A.; Burke, S.; Meng, F.; Thompson, R. C.; Akil, H.; Watson, S. J. Mu, delta, and kappa opioid receptor mRNA expression in the rat CNS: An in situ hybridization study. *J. Comp. Neurol.* **1994**, 350, 412–438.

(38) George, S. R.; Zastawny, R. L.; Brionesurbina, R.; Cheng, R.; Nguyen, T.; Heiber, M.; Kouvelas, A.; Chan, A. S.; Odowd, B. F. Distinct distributions of mu, delta and kappa opioid receptor mRNA in rat brain. *Biochem. Biophys. Res. Commun.* **1994**, 205, 1438–1444.

(39) Saccone, P. A.; Lindsey, A. M.; Koeppe, R. A.; Zelenock, K. A.; Shao, X.; Sherman, P.; Quesada, C. A.; Woods, J. H.; Scott, P. J. H. Intranasal Opioid Administration in Rhesus Monkeys: PET Imaging and Antinociception. *J. Pharmacol. Exp. Ther.* **2016**, 359, 366–373.